Applied Physics Letters

Beta (β) tungsten thin films: Structure, electron transport, and giant spin Hall effect

Cite as: Appl. Phys. Lett. **106**, 182403 (2015); https://doi.org/10.1063/1.4919867
Submitted: 07 April 2015 • Accepted: 25 April 2015 • Published Online: 04 May 2015

Qiang Hao, Wenzhe Chen and Gang Xiao

View Online Export Citation CrossMark

ARTICLES YOU MAY BE INTERESTED IN

Structure and stability of sputter deposited beta-tungsten thin films
Applied Physics Letters **64**, 3231 (1994); https://doi.org/10.1063/1.111318

Phase transformation of thin sputter-deposited tungsten films at room temperature
Journal of Vacuum Science & Technology B: Microelectronics and Nanometer Structures Processing, Measurement, and Phenomena **20**, 2047 (2002); https://doi.org/10.1116/1.1506905

Phase, grain structure, stress, and resistivity of sputter-deposited tungsten films
Journal of Vacuum Science & Technology A **29**, 051512 (2011); https://doi.org/10.1116/1.3622619

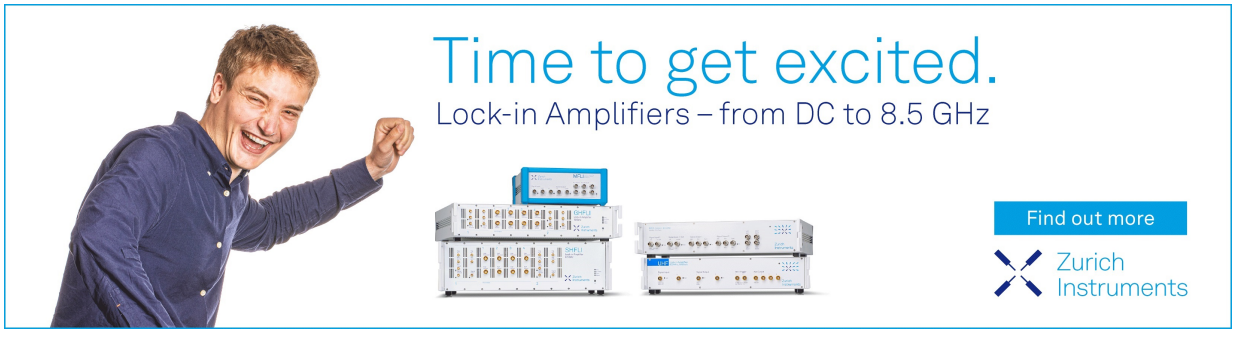

AIP Publishing

© 2015 AIP Publishing LLC.

Beta (β) tungsten thin films: Structure, electron transport, and giant spin Hall effect

Qiang Hao, Wenzhe Chen, and Gang Xiao[a)]
Department of Physics, Brown University, Providence, Rhode Island 02912, USA

(Received 7 April 2015; accepted 25 April 2015; published online 4 May 2015)

We use a simple magnetron sputtering process to fabricate beta (β) tungsten thin films, which are capable of generating giant spin Hall effect. As-deposited thin films are always in the metastable β-W phase from 3.0 to 26.7 nm. The β-W phase remains intact below a critical thickness of 22.1 nm even after magnetic thermal annealing at 280 °C, which is required to induce perpendicular magnetic anisotropy (PMA) in a layered structure of β-W/$Co_{40}Fe_{40}B_{20}$/MgO. Intensive annealing transforms the thicker films (>22.1 nm) into the stable α-W phase. We analyze the structure and grain size of both β- and α-W thin films. Electron transport in terms of resistivity and normal Hall effect is studied over a broad temperature range of 10 K to at least 300 K on all samples. Very low switching current densities are achieved in β-W/$Co_{40}Fe_{40}B_{20}$/MgO with PMA. These basic properties reveal useful behaviors in β-W thin films, making them technologically promising for spintronic magnetic random access memories and spin-logic devices. © *2015 AIP Publishing LLC*. [http://dx.doi.org/10.1063/1.4919867]

Highly resistive beta (β) tungsten characterized by a large spin-orbit coupling (SOC) exhibits giant spin Hall effect (GSHE).[1–3] Its spin Hall angle approaches 0.40,[3] the largest among transition elements, and it converts charge current into spin current efficiently.[3] Robust perpendicular magnetic anisotropy (PMA) has been realized in a layered structure combining the elusive, metastable β-W and a $Co_{40}Fe_{40}B_{20}$ thin film.[3] The GSHE yields, after suitable thermal magnetic annealing, a very low critical current density for magnetization switching.[3] However, fabricating β-W films is challenging. Although W metallization process is used for the very-large-scale-integrated (VLSI) circuits, it is the stable and conductive α-W phase that meets the requirement of semiconductor processing.[4] Tomorrow's spintronic magnetic random access memories (MRAM)[5] and spin-logic devices[6] could increasingly rely on the newly discovered GSHE in β-W films. It is, therefore, imperative to understand the properties and fabrication of the β-W solid. To date, much effort has been made to stabilize the β-W phase.[4,7–15] Nevertheless, very little work is available on the β-W solid in the context of GSHE[1–3] and on its basic properties.

In this work, we prepare a series of β-W thin films with a broad range of thickness (3.0–26.7 nm) using a simple magnetron sputtering process. Based on the process, we achieve PMA and a large spin Hall angle (0.40)[3] in the bulk β-W in a structure of β-W/$Co_{40}Fe_{40}B_{20}$/MgO. We examine the effect of thermal annealing on the structure of the W films. We find that the metastable β-W and β-W/$Co_{40}Fe_{40}B_{20}$/MgO structures can be easily fabricated, making them technologically promising. We measure the temperature dependence of resistivity and normal Hall effect of the β-W films down to the lowest temperature of 10 K. These basic properties of β-W are elucidating in the understanding of this large SOC solid.

[a)]Author to whom correspondence should be addressed. Electronic mail: Gang_Xiao@Brown.edu

We prepare the W films under ambient conditions using a homemade high vacuum magnetron sputtering system equipped with a cryopump. The face-up sputtering guns have a diameter of 5 cm and use an NdFeB permanent magnet ring. The target-substrate distance is 9 cm. The face-down substrates are thermally oxidized single crystal Si wafers (5-cm diameter), which rotate at about 50 rpm during deposition for achieving thickness uniformity. The off-center distance is 3 cm between the center of a substrate and that of a target. The base pressure is less than 2×10^{-8} Torr and the Ar sputtering pressure is ~2.2 mTorr. For the formation of β-W, we apply a low dc sputtering power of only 3 W intermittently to keep a low deposition rate of 0.02 nm/s. The films are patterned using photolithography into standard Hall bars for both Hall effect and resistivity measurements, with longitudinal dimensions of $20 \times 55\ \mu m^2$ in area. In addition to these as-deposited samples, we also prepare a corresponding set of samples that are annealed at 280 °C for 1 min with 2 h of ramping up and 6 h of natural cooling in vacuum (1×10^{-6} Torr) and under a perpendicular magnetic field (0.45 T) to the films. We used the Quantum Design Physical Property Measurement System to measure resistivity and Hall effect as functions of temperature between 5 K and 380 K. The Bruker D8 Discover X-ray Diffraction (XRD) system is used for structural measurement.

Figure 1 shows the XRD patterns for the as-deposited and the annealed W films with thickness in the range of 14.5 to 26.7 nm. All as-deposited films have single phase β-W, which is an A_3B solid with the $A15$ type crystal structure. The annealed films remain in the β-W phase up to a critical thickness (t_c) of 22.1 nm. Above 22.1 nm, films are transformed into the α-W phase, which have the bcc crystal structure. For β-W films, we calculate the average lattice constant based on the (200), (210), and (211) peaks. For α-W films, the lattice constant is obtained from the (110) peak. Figure 2(a) shows the lattice constant as a function of film thickness, which

 © 2015 AIP Publishing LLC

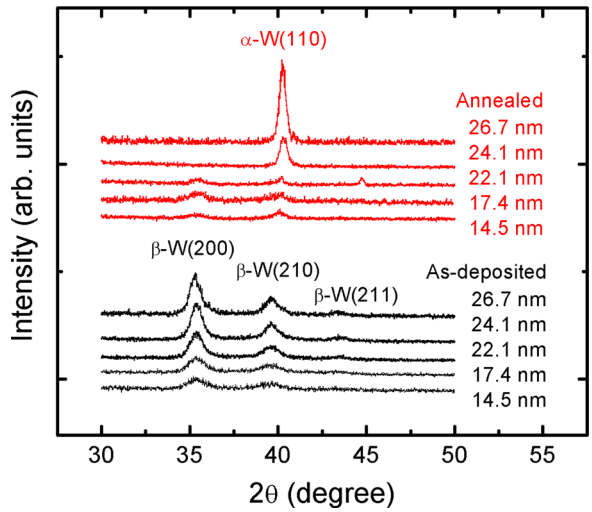

FIG. 1. θ-2θ x-ray diffraction patterns for as-deposited and annealed W thin films with various thicknesses.

reveals clearly the effect of annealing. Up to the largest thickness of 26.7 nm, the lattice constant of the as-deposited β-W films remains unchanged. However, post-annealing and beyond t_c, the lattice constant becomes that of the α structure. Therefore, if the GSHE of β-W is intended for spintronic devices which typically require magnetic thermal annealing, the actual thickness of the β-W film must be smaller than t_c. We note that the spin diffusion length (λ_{sf}) in β-W film[3] is 3.5 nm, which is much smaller than t_c. Therefore, the full strength of the GSHE of β-W film can be exploited as long as thickness is less than t_c, but larger than λ_{sf}.

XRD data provide us with an estimate on the size of crystallites or grain size. According to the Scherrer equation,[16] which relates the grain size to the broadening of a diffraction peak, the average grain size is given by $K\lambda/\beta\cos\theta$, where K is a shape factor (typically about 0.9), λ is the X-ray wavelength, β is the width of a diffraction peak at half maximum intensity, and θ is the Bragg angle. The Scherrer equation remains valid to the extent that the peak broadening is primarily due to the grain size rather than other inhomogeneities. Based on our XRD data, we obtain the grain size estimated using the Scherrer equation, as shown in Fig. 2(b) as a function of W film thickness for the as-deposited and the annealed samples. In both cases, the grain size is smaller than, but increases with, the film thickness. Annealing increases the grain size by about 50%–70%. It is noted the grain size in all samples is much larger (by a factor of 2–4) than the $\lambda_{sf} = 3.5$ nm in β-W.[3] Therefore, λ_{sf} is not predominantly affected by the gain size, but is more dependent on the local structures within the β-W crystallites (such as atomic and lattice disorders).

Next, we focus on the electron transport properties of the films. Figure 3(a) shows the resistivities of the W films as functions of temperature (T = 5 K to 380 K). The as-deposited β-W films (3.0–24.1 nm) are characterized by very large resistivities of 183.5–204.8 $\mu\Omega$ cm at 300 K. Also noteworthy is that the temperature coefficient of resistivity, $(1/\rho)\Delta\rho/\Delta T$, is very small for the β-W films over the whole T range. For example, for the 14.5 nm-thick β-W film, its resistivity remains nearly constant (variation less than 1%) at 190.0 $\mu\Omega$ cm from 5 K to 380 K. This property is advantageous, if β-W is used to generate spin current based on the GSHE. It would mean that the magnetic switching power will not depend on T, hence, providing a wide T range of operation for the spintronic devices.

For a continuous thin film with a thickness t much larger than the effective electron mean free path λ_{eff}, the thin film resistivity can be expressed as[17]

$$\rho(t) = \rho_B + \frac{3}{8}\rho_B\lambda_{eff}/t, \tag{1}$$

where ρ_B is the bulk resistivity. Figure 3(b) shows the resistivities of the β-W thin films versus the inverse thickness ($1/t$). Within the range of 3.0–22.1 nm, Eq. (1) can fit the resistivity data marginally. From the fit, we obtain that $\rho_B(300\,\text{K}) \approx 195 \pm 3\,\mu\Omega$ cm and $\lambda_{eff}(300\,\text{K}) \approx 0.45 \pm 0.26$ nm, $\rho_B(10\,\text{K}) \approx 192 \pm 8\,\mu\Omega$ cm and $\lambda_{eff}(10\,\text{K}) \approx 0.95 \pm 0.52$ nm for the bulk β-W film. The thermally induced resistivity, $\Delta\rho = \rho_B(300\,\text{K}) - \rho_B(10\,\text{K}) < 9\,\mu\Omega$ cm, is insignificant, indicating that the electron-phonon inelastic scattering is relatively weak compared with the disordered elastic scattering. We note that the $\rho_B(300\,\text{K}) \approx 5.33\,\mu\Omega$ cm for the pure α-W bulk solid,[18] which is much smaller than resistivities of any of our β-W thin films. The value λ_{eff} is much smaller than the thickness and the grain size of the films by a factor of 5–10. Therefore, the finite-size effect and the grain boundary scattering are not sufficient to account for the large resistivity of the β-W films. It has been suggested that β-W phase is probably stabilized by small amounts of oxygen.[4,15] Further work, particularly theoretical study, is needed to evaluate whether small amounts of oxygen is responsible for electron disordered scattering either from charge-dependent impurity scattering or spin-orbit scattering. Judging from the large spin Hall angle

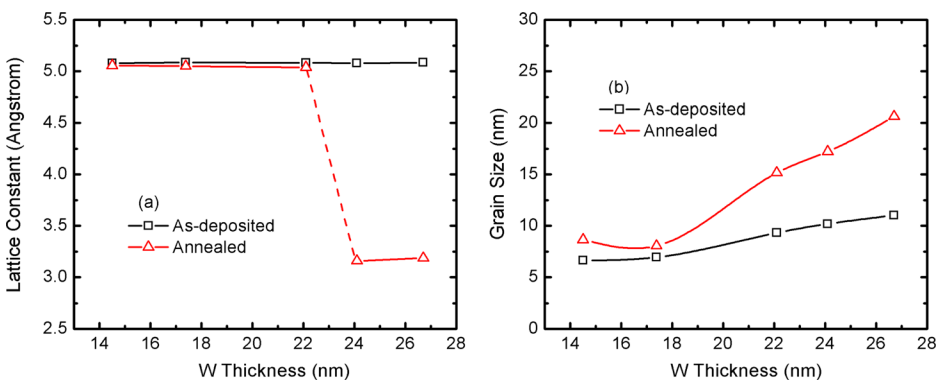

FIG. 2. (a) Lattice constant determined from XRD as a function of W film thickness for as-deposited and annealed samples; (b) Grain size determined by using the Scherrer equation as a function of W film thickness.

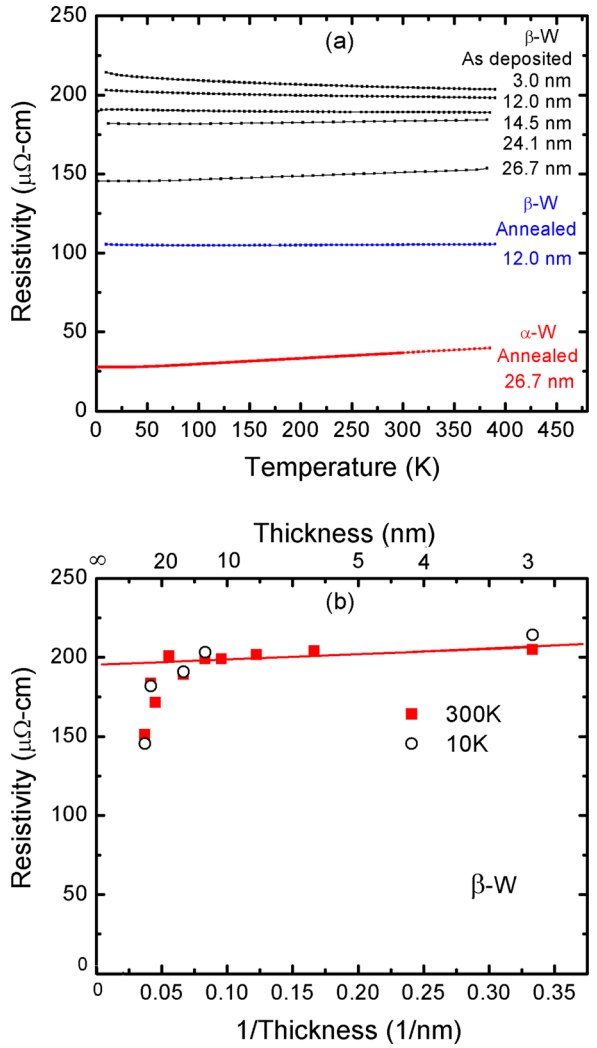

FIG. 3. (a) Temperature dependence of resistivity for β-W and α-W thin films between 10 K and 380 K; (b) Resistivities at 300 K and 10 K versus inverse film thickness ($1/t$) for β-W films (3.0–26.7 nm). The solid straight line is the theoretical fit using Eq. (1) within 3.0 and 22.1 nm based on the finite-size effect of thin film resistivity.

observed in β-W films,[1–3] we conjecture that the disordered spin-orbit scattering plays a significant role in the resistivity of the β-W films. Above 22.1 nm, as shown in Fig. 3(b), the resistivities drop significantly from Eq. (1). We believe that these thicker films may have a small mixture of α-W phase, which has a much smaller resistivity than β-W phase. For the annealed films, we observe that resistivity remains large (100–260 $\mu\Omega$ cm) for films that remain β-W phase.

We note that, when the thickness of β-W is smaller than 14.5 nm, the resistivity of the films is slightly larger at 10 K than at 300 K. This behavior indicates the appearance of a weakly thermally activated electron transport, complicating any analysis on the electron-phonon contribution. Also, in the thin-film limit, e.g., ~3 nm, the thickness is not much larger than the extracted λ_{eff}, and the validity of Eq. (1) is weakened. Therefore, the λ_{eff} value is somewhat uncertain in the thin-film limit.

After annealing, the 24.1 nm and 26.7 nm films are transformed into the α-W phase. We found that $\rho(300\,\mathrm{K}) \approx 36.7$ $\mu\Omega$ cm and $\rho(10\,\mathrm{K}) \approx 27.7$ $\mu\Omega$ cm for the 26.7 nm-thick α-W film. Comparing with β-W, the resistivity of the α-W phase is much more dependent on temperature. For example, in the 26.7 nm-thick α-W film, the thermally induced resistivity, $\Delta\rho = \rho_B(300\,\mathrm{K}) - \rho_B(10\,\mathrm{K}) \approx 9.0$ $\mu\Omega$ cm, indicating a significant contribution from the electron-phonon scattering.

We have also measured the normal Hall effect which is an integral part of the electron transport of a metal. An investigation of both the resistivity and Hall effect and their temperature dependence provides insight into the β-W solid with a strong SOC. Figure 4 shows the temperature dependence of the Hall effect of the β-W and α-W thin films. The Hall coefficient for β-W thin film is $R_H(300\,\mathrm{K}) = -1.62 \times 10^{-8}\,\Omega\,\mathrm{cm/T} = -1.62 \times 10^{-10}$ m^3/C. $R_H(T)$ always carries a negative sign and is linearly dependent on T between 10 K and 300 K. At 10 K, the magnitude of $R_H(10\,\mathrm{K})$ (-1.14×10^{-8} Ω cm/T) is reduced by 30% from the room temperature value. Overall, the charge carriers are predominantly electrons in the β-W thin film. For α-W thin films, $R_H(300\,\mathrm{K})$ is -1.91×10^{-9} Ω cm/T $= -1.91 \times 10^{-11}$ m^3/C, consistent with literature.[19] It carries a negative sign and is about 5 times smaller than the bulk value ($R_H(300\,\mathrm{K}) = +8.6 \times 10^{-11}$ to $+11.8 \times 10^{-11}$ m^3/C).[18,20] $R_H(T)$ for α-W thin films is also linearly dependent on temperature. However, $R_H(T)$ changes sign from negative to positive as temperature is reduced below 130 K, indicating a competition between electron and hole carriers from multi-bands in α-W thin films. The Hall effect data presented in Fig. 4 provide valuable input into any theoretical effort to understand the effects of band structure, scattering mechanisms, and possibly, surface electronic states of β-W and α-W thin films incorporating the inherently strong SOC. Small amounts of oxygen in β-W or α-W thin films may also have some effect on the Hall effect and its temperature dependence.

Using sputtering method described above, we make a layered structure in the form of (t)W/(1.0)$Co_{40}Fe_{40}B_{20}$/(1.6)MgO/(1.0)Ta (number in the units of nm). The (1.0)Ta capping layer is used to prevent the oxidation of the active layers from atmosphere. After annealing, the (1.0)$Co_{40}Fe_{40}B_{20}$ develops PMA,[3] while the W layer remains in β-phase. Figure 5 shows the magnetic switching of the (1.0)$Co_{40}Fe_{40}B_{20}$ layer induced by the spin current generated in the (6.0)β-W layer.

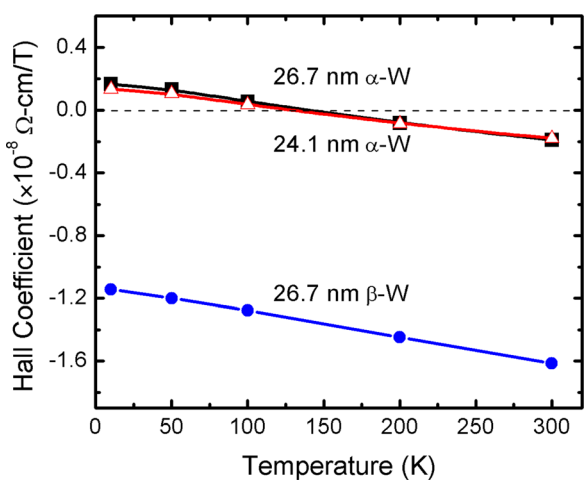

FIG. 4. Temperature dependence of normal Hall coefficient of β-W (26.7 nm) and α-W (24.1 nm and 26.7 nm). Normal Hall effect is measured between −5 T and +5 T. Note the sign change at about 130 K for α-W.

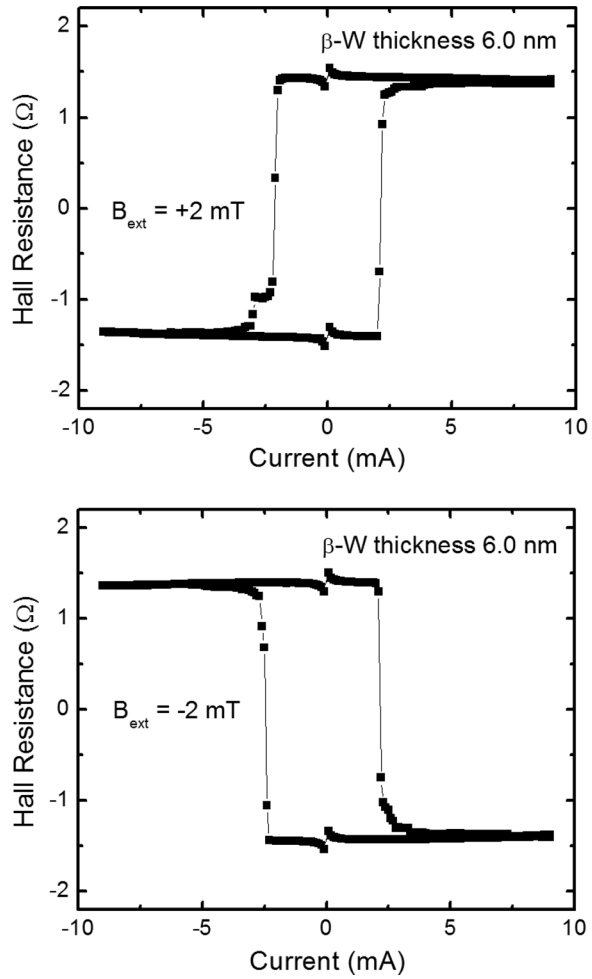

FIG. 5. Current-induced magnetic-switching curves in the (6.0)W/(1.0)$Co_{40}Fe_{40}B_{20}$/(1.6)MgO/(1.0)Ta sample, under an in-plane magnetic field $\mathbf{B_{ext}}$ of +/− 2 mT (+ parallel and − antiparallel to current direction). Magnetic switching in the PMA (1.0)$Co_{40}Fe_{40}B_{20}$ layer is sensed by measuring the anomalous Hall voltage in the layer as current is swept in the Hall bar sample.

We detect the switching by measuring the anomalous Hall effect of the (1.0)$Co_{40}Fe_{40}B_{20}$ layer. Under an in-plane magnetic field of 2 mT, the sample (6.0)W/(1.0)$Co_{40}Fe_{40}B_{20}$/(1.6)MgO/(1.0)Ta can be magnetically switched with a critical current (I_C) of 2.2 mA, corresponding to a critical current density (J_C) of 1.2×10^6 A/cm^2 in the W layer, about 1 order of magnitude smaller than those obtained in other similar structures.[2,5,21,22]

In conclusion, β-W thin films have been fabricated using a simple magnetron sputtering process. The as-deposited films are all in β-W phase from 3.0 to 26.7 nm. In order to obtain PMA in a layered structure of β-W/$Co_{40}Fe_{40}B_{20}$/MgO, high vacuum thermal magnetic annealing is required at a temperature of 280 °C. Upon annealing, β-W is transformed into the α-W phase above a critical thickness of 22.1 nm, which is much larger than the spin diffusion length (3.5 nm) for β-W thin films. The stabilization of β-W up to 22.1 nm after annealing makes it possible to exploit the full GSHE in β-W thin films. In our films, the typical grain size is about one third to one half of the thin film thickness. The room temperature resistivity of the bulk β-W film is 195 $\mu\Omega$ cm and the electron mean free path is very short at 0.45 ± 0.26 nm. Interestingly, the resistivity of β-W is insensitive to temperature and thickness. At 14.5 nm, the temperature coefficient of resistivity is nearly zero between 5 K and 380 K. This property is highly desirable for spintronics applications, since the magnetic switching power from GSHE would not depend on temperature. Finally, the normal Hall coefficient for β-W thin films has been measured between 10 K and 300 K. Although the Hall coefficient has the same magnitude as bulk α-W, it carries a negative sign. This observation provides a useful input into any theory on the electronic structure of β-W incorporating the large SOC. Using our sputtering and magnetic thermally annealing process, PMA and low switching current density can be achieved in the layered structure of β-W/$Co_{40}Fe_{40}B_{20}$/MgO.

This work was supported by Nanoelectronics Research Initiative (NRI) through the Institute for Nanoelectronics Discovery and Exploration (INDEX) and by National Science Foundation through Grant Nos: DMR-1307056 and DMR-1229195.

[1]C.-F. Pai, L. Liu, Y. Li, H. W. Tseng, D. C. Ralph, and R. A. Buhrman, Appl. Phys. Lett. **101**, 122404 (2012).
[2]C.-F. Pai, M.-H. Nguyen, C. Belvin, L. H. Vilela-Leão, D. C. Ralph, and R. A. Buhrman, Appl. Phys. Lett. **104**, 082407 (2014).
[3]Q. Hao and G. Xiao, Phys. Rev. Appl. **3**, 034009 (2015).
[4]P. Petroff, T. T. Sheng, A. K. Sinha, G. A. Rozgonyi, and F. B. Alexander, J. Appl. Phys. **44**, 2545 (1973).
[5]L. Liu, C.-F. Pai, Y. Li, H. W. Tseng, D. C. Ralph, and R. A. Buhrman, Science **336**, 555 (2012).
[6]S. Datta, S. Salahuddin, and B. Behin-Aein, Appl. Phys. Lett. **101**, 252411 (2012).
[7]W. R. Morcom, W. L. Worrell, H. G. Sell, and H. I. Kaplan, Metall. Trans. **5**, 155 (1974).
[8]C. C. Tang and D. W. Hess, Appl. Phys. Lett. **45**, 633 (1984).
[9]D. C. Paine, J. C. Bravman, and C. Y. Yang, Appl. Phys. Lett. **50**, 498 (1987).
[10]I. A. Weerasekera, S. I. Shah, D. V. Baxter, and K. M. Unruh, Appl. Phys. Lett. **64**, 3231 (1994).
[11]S. M. Rossnagel, I. C. Noyan, and C. Cabral, Jr., J. Vac. Sci. Technol., B **20**, 2047 (2002).
[12]D. Choi, B. Wang, S. Chung, X. Liu, A. Darbai, A. Wise, N. T. Nuhfer, K. Barmak, A. P. Warren, K. R. Coffey, and M. F. Toney, J. Vac. Sci. Technol. A **29**, 051512 (2011).
[13]K. Salamon, O. Milat, N. Radic, P. Dubcek, M. Jercinovic, and S. Bernstorff, J. Phys. D: Appl. Phys. **46**, 095304 (2013).
[14]V. N. Volodin, Yu. Zh. Tuleushev, and E. A. Zhakanbaev, J. Surf. Invest.: X-Ray, Synchrotron Neutron Tech. **8**, 169 (2014).
[15]A. J. Narasimham, M. Medikonda, A. Matsubayashi, P. Khare, H. Chong, R. J. Matyi, A. Diebold, and V. P. LaBella, AIP Adv. **4**, 117139 (2014).
[16]A. L. Patterson, Phys. Rev. **56**, 978 (1939).
[17]L. Eckertova, *Physics of Thin Films* (Plenum, New York, 1986), pp 219–233.
[18]*AIP Handbook*, 3rd ed., edited by D. E. Gray (American Institute of Physics, New York, 1972).
[19]Z. Bastl, Thin Solid Films **10**, 311–313 (1972).
[20]*Physical and Chemical Properties of the Elements*, edited by G. V. Samsonov (Naukova Dumka, Kiev, 1965).
[21]X. Qiu, P. Deorani, K. Narayanapillai, K.-S. Lee, K.-J. Lee, H.-W. Lee, and H. Yang, Sci. Rep. **4**, 4491 (2014).
[22]L. Liu, O. J. Lee, T. J. Gudmundsen, D. C. Ralph, and R. A. Buhrman, Phys. Rev. Lett. **109**, 096602 (2012).